Free Radical Biology and Medicine 89 (2015) 883–894

Contents lists available at ScienceDirect

Free Radical Biology and Medicine

journal homepage: www.elsevier.com/locate/freeradbiomed

Original Contribution

# Selective superoxide generation within mitochondria by the targeted redox cycler MitoParaquat

Ellen L. Robb [a], Justyna M. Gawel [b], Dunja Aksentijević [c], Helena M. Cochemé [d], Tessa S. Stewart [a], Maria M. Shchepinova [b], He Qiang [e,f], Tracy A. Prime [a], Thomas P. Bright [a], Andrew M. James [a], Michael J. Shattock [c], Hans M. Senn [b], Richard C. Hartley [b,**], Michael P. Murphy [a,*]

[a] MRC Mitochondrial Biology Unit, Hills Road, Cambridge CB2 0XY, UK
[b] WestCHEM School of Chemistry, University of Glasgow, Glasgow G12 8QQ, UK
[c] King's College London, British Heart Foundation Centre of Research Excellence, The Rayne Institute, St Thomas' Hospital, London SE1 7EH, UK
[d] MRC Clinical Sciences Centre, Imperial College London, Du Cane Road, London W12 0NN, UK
[e] Key Laboratory of Adolescent Health Assessment and Exercise Intervention, Ministry of Education, East China Normal University, Shanghai 200241, China
[f] College of Physical Education and Health, East China Normal University, Shanghai 200241, China

ARTICLE INFO

*Article history:*
Received 24 June 2015
Received in revised form
10 August 2015
Accepted 11 August 2015
Available online 8 October 2015

ABSTRACT

Superoxide is the proximal reactive oxygen species (ROS) produced by the mitochondrial respiratory chain and plays a major role in pathological oxidative stress and redox signaling. While there are tools to detect or decrease mitochondrial superoxide, none can rapidly and specifically increase superoxide production within the mitochondrial matrix. This lack impedes progress, making it challenging to assess accurately the roles of mitochondrial superoxide in cells and *in vivo*. To address this unmet need, we synthesized and characterized a mitochondria-targeted redox cycler, MitoParaquat (MitoPQ) that comprises a triphenylphosphonium lipophilic cation conjugated to the redox cycler paraquat. MitoPQ accumulates selectively in the mitochondrial matrix driven by the membrane potential. Within the matrix, MitoPQ produces superoxide by redox cycling at the flavin site of complex I, selectively increasing superoxide production within mitochondria. MitoPQ increased mitochondrial superoxide in isolated mitochondria and cells in culture ~a thousand-fold more effectively than untargeted paraquat. MitoPQ was also more toxic than paraquat in the isolated perfused heart and in *Drosophila in vivo*. MitoPQ enables the selective generation of superoxide within mitochondria and is a useful tool to investigate the many roles of mitochondrial superoxide in pathology and redox signaling in cells and *in vivo*.



Superoxide production from respiratory complexes is a major source of mitochondrial reactive oxygen species (ROS) [1,2]. Within the matrix, superoxide is rapidly converted by Mn superoxide dismutase (MnSOD) to hydrogen peroxide, which contributes to oxidative damage in a range of pathologies, including ischemia/reperfusion injury, diabetes and neurodegeneration [3–5]. Mitochondria-derived hydrogen peroxide is also a signaling molecule that transduces redox signals by modifying the activity of redox-sensitive proteins [6–8]. However, our understanding of the nuanced roles of mitochondrial superoxide in pathology and normal physiology is limited, making this an area of intense current activity.

To investigate the impact of mitochondrial superoxide on pathology and redox signaling, it is vital to be able to manipulate its levels within mitochondria in cells and *in vivo*. Selectively decreasing mitochondrial superoxide is possible by increasing expression of the endogenous antioxidant enzyme MnSOD [9,10], or through the use of targeted antioxidants (e.g. MitoSOD [11]). In contrast, few methods exist to augment mitochondrial ROS production selectively. The homozygous deletion of MnSOD elevates superoxide levels in mice at birth, but is lethal within a few days [12]. In MnSOD (+/−) mice, mitochondrial function is disrupted throughout their lifespan, but this may lead to compensatory changes that mask the effects of superoxide, and furthermore the relationship between MnSOD expression and matrix superoxide levels is unclear [13,14]. Finally, many physiological and pathological consequences of superoxide occur following its transformation to hydrogen peroxide, and the rate and extent of this transformation are affected by MnSOD level [15,16]. Mitochondrial

* Corresponding author.
** Corresponding author.
*E-mail addresses:* Richard.Hartley@glasgow.ac.uk (R.C. Hartley), mpm@mrc-mbu.cam.ac.uk (M.P. Murphy).

http://dx.doi.org/10.1016/j.freeradbiomed.2015.08.021

superoxide generation can be increased by treatment with respiratory inhibitors such as rotenone or antimycin [1], but these disrupt the membrane potential, and ATP, NADH and NADPH synthesis, making interpretation of experimental results challenging. Exogenous redox cyclers such as paraquat (PQ) [17] or menadione [18] generate superoxide *in vivo*, however this occurs in many cell compartments, making it difficult to distinguish effects due to mitochondrial superoxide.

Therefore we cannot currently increase mitochondrial superoxide selectively in cells or *in vivo*. The ability to enhance superoxide production specifically within mitochondria would transform the investigation of ROS-mediated damage and signaling, and also facilitate the development of better detection methods. What is required is a small molecule that generates superoxide only in the mitochondrial matrix, with negligible production in other parts of the cell. To generate superoxide we chose derivatives of the viologen PQ (1,1'-dimethyl-4,4'-bipyridinium dichloride), a herbicide widely used to increase superoxide production in isolated mitochondria, cells and model organisms [14,17,19]. Within mammalian mitochondria, the one-electron reduction of PQ at the flavin site of complex I generates the radical monocation $PQ^{\bullet+}$, which goes on to react very rapidly ($k \sim 7.7 \times 10^8\ M^{-1}\ s^{-1}$) with oxygen to produce superoxide [17,19,20]. Although PQ can increase mitochondrial superoxide formation *in vivo*, its mitochondrial uptake is by a slow and poorly characterized process [19]. As a result, very high PQ concentrations are required for mitochondrial effects, leading to extensive superoxide production at non-mitochondrial sites [21,22]. Therefore here we sought to develop PQ derivatives that would be selectively and rapidly accumulated by mitochondria, thereby generating superoxide only within the organelle.

Due to their high membrane potential, mitochondria naturally accumulate cations which either diffuse directly through the mitochondrial inner membrane or cross the membrane facilitated by a protein [23]. Although PQ is a cation, its high surface charge and polar interface with water greatly increase the energetic cost for its movement through the hydrophobic core of the mitochondrial inner membrane [24]. To mitigate this energetic penalty, we tested two strategies. The first was to increase the hydrophobicity of the viologen moiety of PQ so as to make its partitioning into the membrane less unfavorable [23]. The second was to conjugate PQ to the lipophilic triphenylphosphonium (TPP) cation, which accumulates in mitochondria in response to the mitochondrial membrane potential. This strategy has been used extensively to target small molecules to mitochondria in cells, tissues and whole animals [23–26]. Here we report a mitochondria-targeted compound, MitoParaquat (MitoPQ) (Fig. 1), which can be used to selectively increase superoxide production within the mitochondrial matrix in cells and *in vivo*.

## 1. Materials and methods

### 1.1. Chemical syntheses

The synthesis of the compounds investigated is outlined in Fig. 2A and the experimental details are given in the Supplementary Information. The structures of the viologens are shown in Fig. 2B and of the monoalkylated bipyridines in Fig. 2C.

### 1.2. Ethics statement

All experiments were approved by the institutional ethical review committee and conform to the UK Home Office Guidance on the Operation of the Animals Scientific Procedures Act 1986 (HMSO). All procedures were performed in accordance with the *Guide for the Care and Use of Laboratory Animals*.

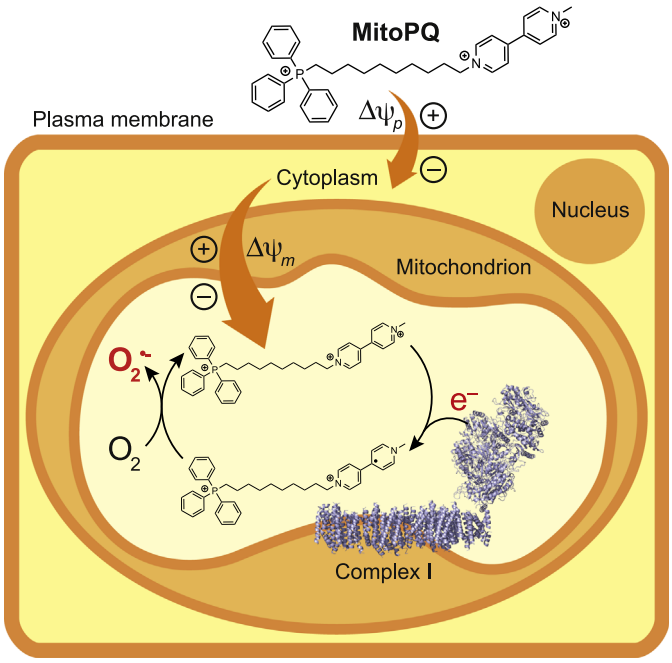


**Fig. 1.** Rationale for the development of MitoParaquat. MitoParaquat (MitoPQ) is composed of a redox cycling paraquat moiety, and a hydrophobic carbon chain linking it to a mitochondria-targeting triphenylphosphonium cation. MitoPQ is accumulated by mitochondria driven by the plasma ($\Delta\psi_p$) and mitochondrial ($\Delta\psi_m$) membrane potentials. Within the matrix, the dicationic viologen component of MitoPQ is reduced to a radical monocation by one-electron reduction at the flavin site of complex I. The radical monocation then reacts very rapidly with $O_2$ to generate superoxide. This localized redox cycling leads to the selective production of superoxide within the mitochondrial matrix.

### 1.3. Mitochondrial preparations and incubations

Mitochondria were prepared from the livers and hearts of female Wistar rats of 10 to 12 weeks of age (Charles River, UK). Animals were killed by stunning followed by cervical dislocation, and the liver and heart were removed to ice-cold buffer. Rat liver mitochondria (RLM) were isolated by homogenization and differential centrifugation at 4 °C in buffer containing 250 mM sucrose, 5 mM Tris-Cl, and 1 mM EGTA (pH 7.4). Rat heart mitochondria (RHM) were isolated in the same buffer supplemented with 0.1% (w/v) fatty acid-free bovine serum albumin. Protein content of the mitochondrial preparations was determined using the biuret assay with bovine serum albumin as a standard. Mitochondrial incubations were performed in KCl buffer [120 mM KCl, 10 mM HEPES, 1 mM EGTA (pH 7.2)], unless stated otherwise. Bovine heart mitochondrial membranes were prepared as described [27] and incubated at 0.2 mg protein/mL in KCl buffer.

### 1.4. Measurement of mitochondrial uptake of compounds by RP-HPLC

RLM (1 mg protein/mL) were incubated in 4 mL KCl buffer supplemented with 5 mM glutamate/malate, the various monoalkylated bipyridines or viologens, and methyltriphenyl phosphonium (TPMP) ± *p*-trifluoromethoxyphenylhydrazone (FCCP) (1 μM) with shaking at 30 °C. After 3 min mitochondria were pelleted by centrifugation (7500 x g, 10 min) and the supernatants were collected and diluted with 100% acetonitrile (ACN), 0.1% trifluoroacetic acid (TFA) to 25% ACN. Mitochondrial pellets were extracted by vortexing in 250 μL 100% ACN, 0.1% TFA followed by

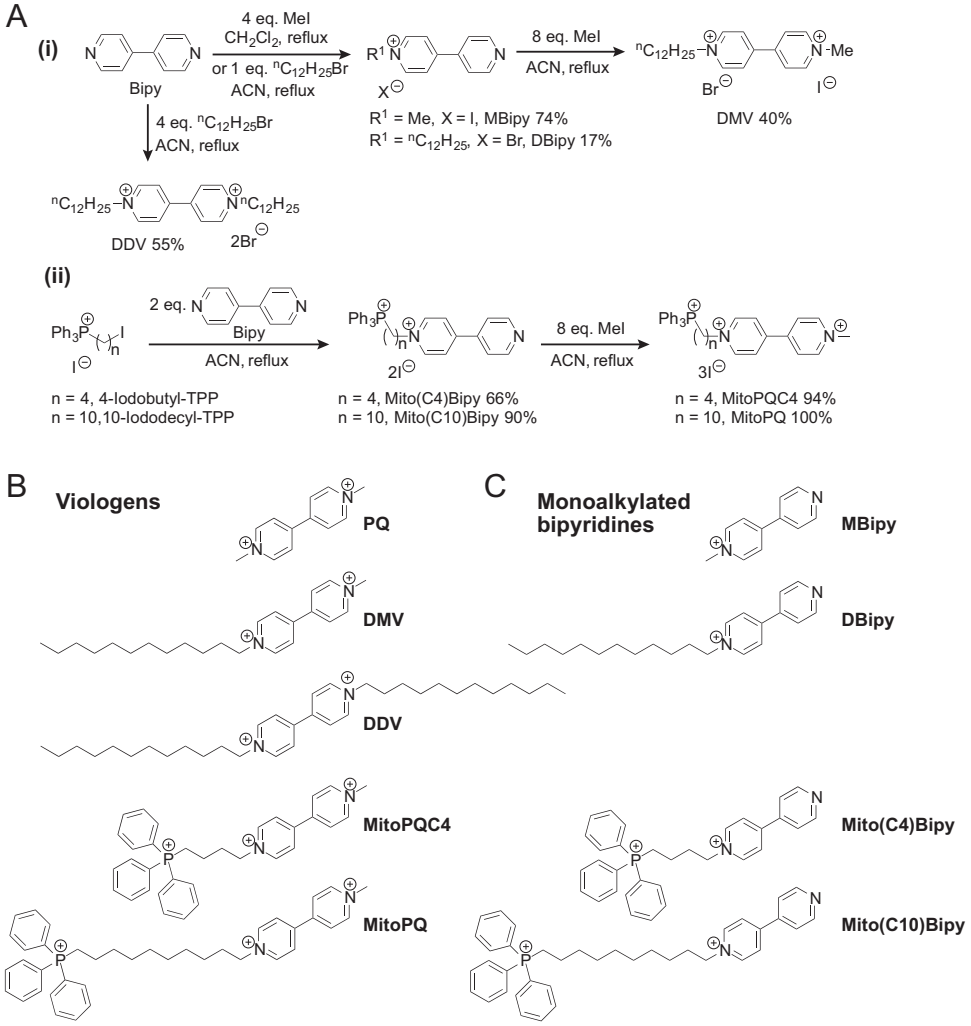


**Fig. 2.** Synthesis and structures of the investigated viologens and monoalkylated bipyridines. (A) Synthetic schemes for: (i) viologens and monoalkylated bipyridines; (ii) viologens and monoalkylated bipyridines conjugated to TPP. ACN, acetonitrile; Me, methyl; Bipy, bipyridine. (B) Viologens: paraquat (PQ), dodecyl methyl viologen (DMV), didodecyl viologen (DDV), Mito(C4)paraquat (MitoPQC4), Mito(C10)paraquat (MitoPQ). (C) Monoalkylated bipyridines: *N*-methylbipyridinium (MBipy), *N*-dodecylbipyridinium (DBipy), Mito(C4)bipyridinium (Mito(C4)Bipy), Mito(C10)bipyridinium (Mito(C10)Bipy).

centrifugation (7500 x g, 10 min) to pellet protein following which the extract was diluted with 0.1% TFA in water to 25% ACN. All samples were filtered through a 0.22 μm syringe-driven polyvinylidene difluoride filter (Millex, Millipore) and 1 mL was separated by RP-HPLC performed using a Gilson 321 pump fitted with a C18 column (Jupiter 300 A, Phenomenex) and a Widepore C18 guard column (Phenomenex). HPLC buffers A (0.1% TFA) and B (90% ACN and 0.1% TFA) were used to generate a gradient: 0–2 min, 5% B; 2–17 min, 5-100% B; 17–19 min, 100% B; 19–22 min 100–5% B with a flow rate of 1 mL/min. Peaks were detected by absorbance at 220 nm (UV/Vis 151; Gilson) and Chart 5 software (AdInstruments) was used to calculate the peak areas. The accumulation ratios (ACRs) of the monoalkylated bipyridines or viologens between the mitochondrial pellets and supernatants were calculated by normalizing the ratios of the peak areas to their corresponding volumes: 0.6 μL/mg protein for the mitochondrial matrix and 4 mL for the supernatant.

### 1.5. Cell culture

C2C12 (mouse myoblasts cell line; European Collection of Animal Cell Cultures), and HCT116 (human colon cancer cell line; American Type Culture Collection) cells were maintained at 37 °C in a humidified 5% $CO_2$ incubator. C2C12 cells were cultured in low glucose (1000 mg/mL) Dulbecco's modified Eagle's medium (DMEM; Invitrogen) supplemented with 10% (v/v) fetal calf serum, 100 U/mL penicillin and 100 μg/mL streptomycin. HCT116 cells were cultured in high glucose (4500 mg/mL) DMEM (Invitrogen) supplemented with 10% (v/v) fetal calf serum, 100 U/mL penicillin and 100 μg/mL streptomycin. Both cell lines were routinely passaged and maintained at sub-confluence. To assess toxicity, C2C12 or HCT116 cells were seeded in 96 well plates at 10 or $15 \times 10^6$ cells per well, respectively. After 6 h fresh medium containing the test compound was added, and after 24 h cell viability was evaluated by measuring lactate dehydrogenase (LDH) release into the medium using the Roche LDH Cytotoxicity Detection Kit, according to the manufacturer's instructions.

### 1.6. Detection of superoxide

Superoxide production in bovine heart mitochondrial membranes was detected by measuring SOD-sensitive coelenterazine chemiluminescence (2 μM; Calbiochem) [28] detected in a luminometer (Berthold AutoLumatPlus LB 953) with 5 s cumulative readings taken every 30 s over 5 min incubations at 30 °C [29]. For incubations with intact mitochondria and cells, aconitase activity was used to infer superoxide production. Following incubation with test compounds, mitochondria were harvested by

centrifugation (7500 x g, 1 min) and cells were harvested by scraping followed by centrifugation (7500 x g, 1 min). Pellets were resuspended in 50 mM Tris-Cl (pH 7.4), 0.6 mM $MnCl_2$ and 2 mM sodium citrate to prevent further aconitase inactivation, lysed by sonication ($10 \times 1$ s pulse; Q700 sonicator, Qsonica), and snap frozen on dry ice and stored at −80 °C until they were thawed rapidly at 30 °C just before assay. Aconitase activity was measured by a coupled enzyme assay and monitored spectrophotmetrically (SpectraMax Plus 384; Molecular Devices) as the production of NADPH at 340 nm [29,30].

### 1.7. Confocal imaging of ROS production within cells

In C2C12 myoblasts, mitochondrial superoxide and hydrogen peroxide production were monitored by live cell imaging using the fluorescent dye MitoSOX (Invitrogen). Nuclei were visualized by staining with Hoechst 33342 (Invitrogen). C2C12 cells were plated overnight on glass-bottomed culture dishes (MatTek). Cells were preloaded with 500 nM MitoSOX and Hoechst 33342 (500 ng/mL) for 10 min in complete growth medium prior to imaging. Cells were washed three times with Krebs buffer immediately prior to imaging. Cells were maintained in Krebs buffer at 37 °C on the temperature-controlled stage of a Nikon Eclipse Ti confocal microscope for the duration of the experiment. Images were captured using a 60x oil immersion lens every 30 s over 20 min. Oxidized MitoSOX was visualized following excitation at 510 nm and emission collected with a LP 560 nm filter. Hoechst 33342 was visualized by excitation at 405 nm and emission collected using a DAPI filter set. Individual cells were tracked through time, and fluorescence intensity was analyzed using Fiji imaging processing and analysis software.

### 1.8. Detection of hydrogen peroxide

The rate of hydrogen peroxide efflux from RHM was assayed using a fluorometric plate reader (SpectraMax GeminiXS; Molecular devices). RHM (0.2 mg protein/mL) were incubated with 50 μM Amplex Red reagent (Invitrogen), 5 U/mL horseradish peroxidase, and 5 mM glutamate/malate at 30 °C. Fluorescence of resorufin was detected by excitation at 570 nm and emission at 585 nm and the response was calibrated against hydrogen peroxide standards in the presence of RHM.

### 1.9. Western blotting

For peroxiredoxin 3 detection, RHM (2 mg protein/mL) were incubated for 3 min at 30 °C in KCl buffer respiring on 5 mM glutamate/malate, supplemented with MitoPQ, PQ or vehicle control. At the end of the incubation 100 mM *N*-ethylmaleimide (NEM) was added and the incubation continued for a further 5 min. Mitochondria were then pelleted by centrifugation (7500 x g, 3 min) and the pellet re-suspended in loading buffer lacking reductant and 20 μg protein separated on a non-reducing 12% SDS-PAGE gel (BioRad). Proteins were then transferred to a PVDF membrane using a BioRad TurboBlot transfer apparatus. Equal protein loading and transfer were verified with Memcode reversible protein stain following the manufacturer's protocol (Pierce Biotechnology). Membranes were blocked with Odyssey Blocking Buffer (LI-COR) for 2 h at room temperature. Incubation with anti-peroxiredoxin 3 (Prdx3; rabbit polyclonal; 1:1000 v/v dilution; ThermoFisher Scientific) was performed overnight at 4 °C. The membranes were visualized using the Odyssey infrared imaging system from LI-COR Biosciences.

For MnSOD detection, C2C12 cells were lysed in ice-cold buffer containing 10 mM Tris pH 8.0, 150 mM NaCl, 2 mM EDTA, 2 mM dithiothreitol, 0.4 mM phenylmethylsulfonylfluoride, 40% (v/v) glycerol and 0.5% (v/v) NP40 for 1 h. Samples were sonicated ($10 \times 1$ s; Q700 sonicator, Qsonica). Cell lysates were centrifuged (13,000 x g for 10 min at 4 °C) and the protein concentration of the resulting supernatant was determined using the bicinchoninic protein assay (Pierce Biotechnology) with bovine serum albumin as a standard. Supernatant (15 μg protein) was run on a 12% SDS-PAGE gel (BioRad) under reducing conditions. Proteins were then transferred to PVDF and assessed for MnSOD or VDAC using anti-MnSOD (rabbit polyclonal; 1:5000 v/v dilution; Abcam) or anti-VDAC (rabbit polyclonal; 1:1000 v/v dilution; Abcam) as described above for Prdx3. Memcode reversible protein stain was used to assess protein loading and transfer.

### 1.10. Isolated perfused mouse heart experiments

C57BL/6J male mice (~25 g, Charles River, UK) were kept in individually ventilated cages with a 12 h light-dark cycle, controlled humidity and temperature (20–22 °C), fed standard chow and water *ad libitum*. Mice were administered terminal anesthesia *via* intra-peritoneal pentobarbitone injection (~140 mg/kg body weight). Beating hearts were rapidly excised, cannulated and perfused in isovolumic Langendorff mode at 80 mm Hg pressure maintained by a STH peristaltic pump controller feedback system (AD Instruments, UK), with Krebs-Henseleit (KH) buffer continuously gassed with 95% $O_2$/5% $CO_2$ (pH 7.4, 37 °C) containing (in mM): NaCl 116, KCl 4.7, $MgSO.7H_2O$ 1.2, $NaHCO_3$ 25, $KH_2PO_4$ 1.2, $CaCl_2$ 1.4, glucose 11 [31]. Hearts were continuously paced at ~550 bpm and cardiac function was assessed using a fluid-filled cling-film balloon inserted into left ventricle (LV) connected via a line to a pressure transducer and a Powerlab system (AD Instruments, UK). The volume of the intraventricular balloon was adjusted using a 1.0 mL syringe to achieve an initial LV diastolic pressure (LVDP) of 4–9 mmHg [31]. Functional parameters (systolic pressure, end diastolic pressure, heart rate, coronary flow, perfusion pressure) were recorded using LabChart software v.7 (AD Instruments, UK) throughout the experiment [31]. LVDP was calculated from the difference between systolic (SP) and diastolic pressures (DP). After 20 min equilibration, hearts were randomized into three groups ($n=6$ in each group) for a further 20 min treatment with: 50 μM PQ, MitoPQ or TPMP in the perfusate. At the end of all perfusion protocols, hearts were immediately snap frozen using Wollenberger tongs pre-cooled in liquid nitrogen and stored at–80 °C until further analysis.

### 1.11. Drosophila maintenance and experiments

Wild-type *Drosophila melanogaster* (*white Dahomey* stock) were maintained on standard sugar-yeast-agar medium at 25 °C, 65% humidity on a 12:12 h light:dark cycle [32]. Experimental flies were raised at constant density from a synchronized egg collection. 7 day old females were microinjected under gentle $CO_2$ anesthesia using a PicoSpritzer III (Parker) as previously described [33], except that the injection solution contained 10% v/v EtOH or PQ/MitoPQ from an EtOH stock solution in Ringers buffer [182 mM KCl, 46 mM NaCl, 3 mM $CaCl_2$, 10 mM Tris-base; pH 7.2 HCl] supplemented with 1 mg/mL Brilliant Blue dye. Following recovery, injected flies were returned to vials of food, incubated at 25 °C, and their survival monitored. A total of ~60–80 flies were injected per condition.

### 1.12. Statistical analysis and experimental design

Data were expressed as mean with S.D. or S.E.M., and *P* values calculated using a two-tailed Student's t-test for pairwise comparisons. One-way analysis of variance (ANOVA) followed by Tukey's post-hoc test was used for multiple comparisons. Statistical

analyses were performed using GraphPad Prism v.6 software.

## 2. Results and discussion

### 2.1. Synthesis and hydrophobicity of viologens and monoalkylated bipyridines

The poor uptake by PQ into mitochondria may be due to the energetic cost of crossing the hydrophobic core of the mitochondrial inner membrane. One way to mitigate this may be to increase the hydrophobicity of the PQ derivative, as this greatly enhances the uptake of other dications into mitochondria [24]. We first increased the hydrophobicity of the viologen core of PQ by adding one or two dodecyl groups to generate dodecyl methyl viologen (DMV) and didodecyl viologen (DDV) with the hope of thereby decreasing the energy for uptake (Fig. 2B). In an alternative strategy, we also conjugated a viologen to a TPP cation (Fig. 2B), which has been widely used to drive uptake into mitochondria of many molecules, including relatively polar moieties (e.g. [34]) (Fig. 2B). Furthermore, as increasing the hydrophobicity of the TPP conjugate enhances the uptake of conjugated polar moieties, we made viologens conjugated to TPP by a 4-carbon linker (MitoPQC4), and with a more hydrophobic 10-carbon linker (MitoPQ) (Fig. 2B).

We also considered that as the double charge on PQ is likely to be a major impediment to uptake, a monocation such as a monoalkyl bipyridine should be taken up more readily and could be more effective at increasing mitochondrial superoxide than an impermeable viologen. Although protonated monoalkylbipyridines will redox cycle as effectively as viologens [35,36] at low pH their low $pK_a$ (~2.7) means they are far more difficult to reduce than PQ at neutral pH ($E_m$ ~ −800 mV [35] against $E_m$ = −446 mV for PQ [36–38]). To assess whether monoalkylated bipyridines could be effective mitochondrial redox cyclers we made *N*-methylbipyridinium (MBipy) and the more hydrophobic *N*-dodecylbipyridinium (DBipy) (Fig. 2C). To assess whether monoalkylated bipyridines could be effective mitochondrial redox cyclers we made *N*-methylbipyridinium (MBipy) and the more hydrophobic *N*-dodecylbipyridinium (DBipy) (Fig. 2C). We also made monoalkylated bipyridines conjugated to a TPP cation by a 4-carbon linker (Mito(C4)Bipy), and one with a more hydrophobic 10-carbon linker (Mito(C10)Bipy) (Fig. 2C).

As the relative hydrophobicities of these compounds is a major determinant of mitochondrial uptake [24], we next compared their retention times by RP-HPLC on a C18 column to that of TPMP as an internal standard (Fig. 3). The order of hydrophobicity is: MitoPQC4 < Mito(C4)Bipy < MitoPQ < Mito(C10)Bipy < TPMP < DMV < DBipy < DDV. Therefore we have a series of viologens and monoalkyl bipyridines with a range of hydrophobicities that can be tested to assess their ability as redox cyclers within mitochondria.

### 2.2. Redox cycling by viologen and monoalkylated bipyridines

Redox cycling by PQ relies on its reduction potential ($E_m$ = −446 mV [36]) allowing it to transfer electrons from the flavin mononucleotide (FMN) site of complex I to oxygen. As varying the alkyl substituents of dialkylbipyridiniums does not alter the reduction potential [36], all our viologen derivatives can in principle redox cycle. However, to be effective redox cyclers within mitochondria, the viologen and monoalkylated bipyridines in Fig. 2 have to access the FMN site of complex I [19,20] (Fig. 1). As this interaction might be disrupted by the bulky alkyl or TPP groups, we next determined whether the viologen and monoalkylated bipyridines could generate superoxide from complex I *in vitro* using mitochondrial membranes incubated with NADH and rotenone (Fig. 4). These membranes are fragmented and therefore uptake across a membrane is not required to access complex I [27]. Superoxide production was detected by the SOD-sensitive chemiluminescence of coelenterazine (CLZ) [28]. NADH and rotenone led to a basal level of superoxide production that was greatly enhanced by PQ and to similar extents by MitoPQC4 and MitoPQ (Fig. 4). DDV and the monoalkylated bipyridines MBipy and DBipy led to a smaller increase in superoxide production over that of NADH, while DMV disrupted complex I, as even basal NADH-dependent superoxide formation was lost (Fig. 4A). In all cases, superoxide production was negligible in the absence of respiratory substrate (data not shown). To facilitate comparison, we subtracted the background superoxide production, showing that the viologens PQ, MitoPQC4 and MitoPQ generated similar high levels of superoxide from complex I, while the alkylated viologen DDV was far less effective (Fig. 4B). All the monoalkylated bipyridines were ~4–15-fold less effective than viologens at generating superoxide. As only a tiny fraction (< < 0.1%) will be protonated at physiological pH (pKa ~2.7) the level of redox cycling is unexpectedly high, perhaps due to an increase in the $pK_a$ of the monoalkylbipyridine upon interacting with the FMN site of complex I.

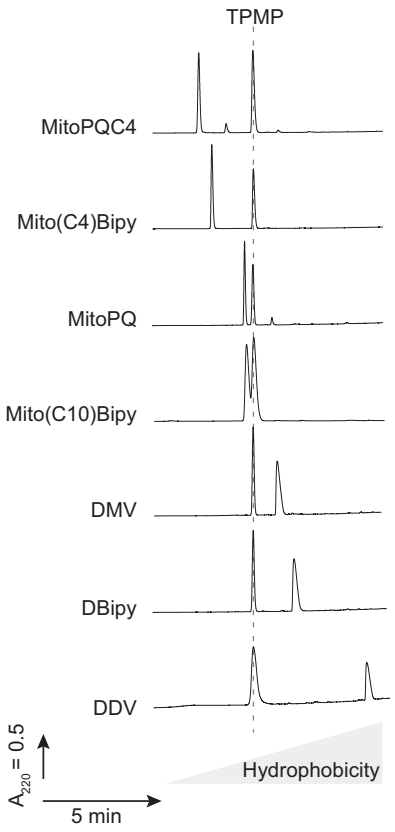


**Fig. 3.** Relative hydrophobicities of MitoPQ and the investigated monoalkylated bipyridines and viologens. The indicated compounds (10 nmol) were mixed with 10 nmol TPMP and separated by RP-HPLC on the indicated gradient of increasing hydrophobicity (Buffer *B*=90% ACN, 0.1% TFA). Compound elution was detected by absorbance at 220 nm and compared to that of TPMP as an internal standard (dashed line).

Therefore we have generated two viologen derivatives conjugated to the TPP cation that redox cycle as well as unmodified PQ, making them potential mitochondria-targeted redox cyclers. In addition, we have made monoalkylated bipyridines that are less effective redox cyclers, but which may still be useful should

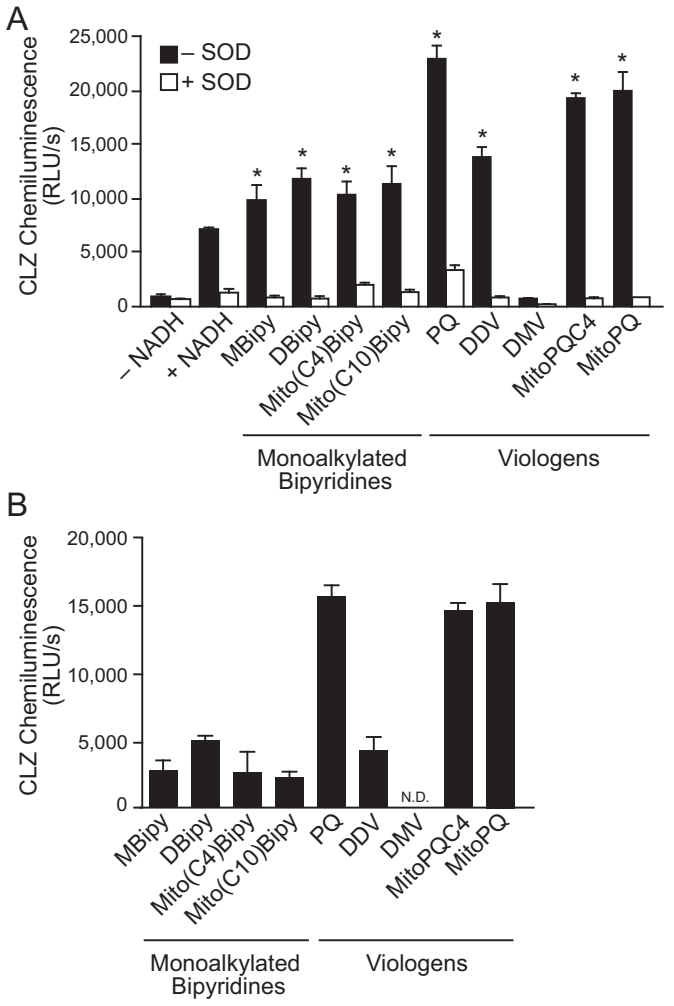


**Fig. 4.** Superoxide generation by redox cycling at complex I in mitochondrial membranes. (A) Superoxide production in bovine heart mitochondrial membranes measured by the CLZ chemiluminescence assay. Membranes were incubated with 1 mM NADH and rotenone (4 μg/mL), and supplemented with Cu,Zn-SOD (100 U/mL) and 1 μM viologens or monoalkylated bipyridines as indicated. Data are means ± S.D. of three independent experiments. $^*p < 0.05$ compared to NADH/rotenone by Student's t test. (B) The rates of superoxide production corrected for that in the presence of SOD.

greater mitochondrial uptake compensate for diminished redox cycling.

### 2.3. MitoPQ is accumulated by energized mitochondria

To enhance superoxide production in mitochondria over PQ, the newly developed compounds have to accumulate rapidly within the matrix in response to the membrane potential (Fig. 1). Therefore we next measured their uptake by energized mitochondria (Fig. 5). After incubation with MitoPQ and TPMP, mitochondria were pelleted and assessed by RP-HPLC, showing extensive uptake of both MitoPQ and TPMP, which was decreased by the uncoupler FCCP (Fig. 5A). To quantify uptake, we also measured the accumulation ratio (ACR), that is the relative amounts of the compounds in the mitochondria and supernatant. Both TPMP and MitoPQ had substantial ACRs which were decreased by FCCP (Fig. 5B). Assessment of the other compounds in the same way showed that DMV, DBipy, and the TPP-conjugated derivative Mito (C10)Bipy were all accumulated by energized mitochondria (Fig. 5B). Interestingly, while MitoPQ and Mito(C10)Bipy were taken up, MitoPQC4 and Mito(C4)Bipy were not, consistent with uptake requiring the hydrophobicity provided by the ten carbon linker to counteract the polar viologen or monalkyl bipyridine moiety.

The uptake of all the monoalkylated bipyridines, including those conjugated to TPP, was lower than for TPMP. That DMV and DDV are taken up, while PQ is not [19], indicates that increasing the hydrophobicity of the doubly charged viologen core does enhance passage through the mitochondrial inner membrane. Therefore we have redox cycling viologens that are taken up into mitochondria to a far greater extent than PQ [19].

### 2.4. MitoPQ stimulates hydrogen peroxide production by isolated mitochondria

We next investigated whether the compounds taken up by energized mitochondria could initiate redox cycling within the matrix. MitoPQ significantly increased hydrogen peroxide production, the product of superoxide dismutation, from heart mitochondria (Fig. 6A). When this analysis was extended to the other compounds it showed that, as expected [19], similar concentrations of PQ were ineffective and that DBipy was the only other compound to increase hydrogen peroxide efflux, albeit to a smaller extent than for MitoPQ (Fig. S1). Therefore, MitoPQ was by far the

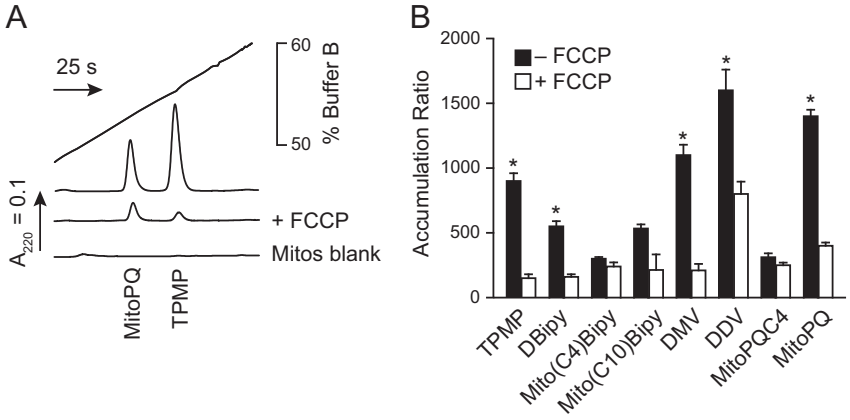


**Fig. 5.** Uptake of compounds by energized mitochondria. (A) RP-HPLC analysis of mitochondrial uptake of TPMP and MitoPQ. Rat liver mitochondria were incubated with succinate (5 mM), rotenone (4 μg/mL), and with 5 μM MitoPQ and 5 μM TPMP ± 500 nM FCCP. After incubation the mitochondria were pelleted by centrifugation and the supernatant retained, the pellets were extracted and TPMP and MitoPQ were detected by RP-HPLC. The panel shows a typical experiment repeated 3 times. (B) Accumulation ratios for compounds in mitochondria. The indicated compounds (5 μM) were incubated with mitochondria as above with 5 μM TPMP ± FCCP. The ratio of the amounts present in the pellets and supernatants were used to determine an accumulation ratio (ACR). All data shown are the means ± S.D. of three independent experiments. $^*p < 0.05$ relative to the + FCCP condition by ANOVA with Tukey's *post hoc* test.

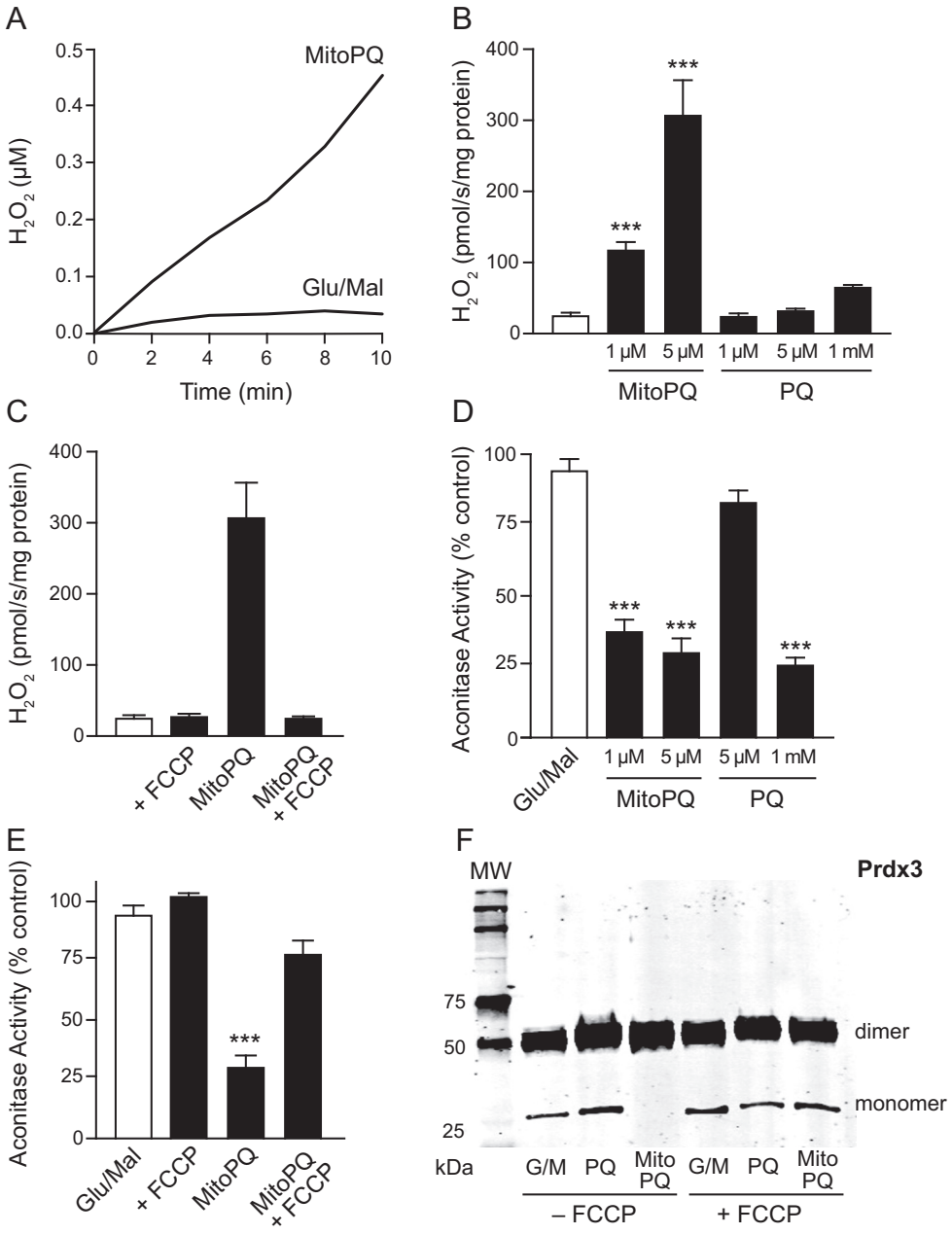


**Fig. 6.** MitoPQ increases superoxide generation within isolated mitochondria. (A) Hydrogen peroxide efflux from heart mitochondria respiring on glutamate/malate was measured in the presence and absence of 5 μM MitoPQ. (B) Hydrogen peroxide efflux from mitochondria in the presence of the indicated compound was measured as in (A). (C) Effect of FCCP (500 nM) on hydrogen peroxide efflux from mitochondria in the presence of MitoPQ. (D, E). Aconitase inactivation within mitochondria by MitoPQ. Rat heart mitochondria were incubated at 30°C with glutamate/malate, supplemented with PQ or MitoPQ ± FCCP (500 nM) as indicated, then aconitase activity was measured. (F) Peroxiredoxin 3 (Prdx3) dimerization induced by MitoPQ in mitochondria. Rat heart mitochondria were incubated with glutamate and malate in the presence of 5 μM PQ or MitoPQ ± 500 nM FCCP, as indicated. Then Prdx3 monomers and dimers were then separated by non-reducing SDS-PAGE and detected by immunoblotting. Data in (B – E) are means ± S.D. of three independent experiments. $^{***}p < 0.001$ relative to control incubations (open bars) by Student's t test.

most effective generator of hydrogen peroxide by isolated mitochondria, presumably due to its membrane potential-dependent accumulation (Fig. 5) and its redox cycling at complex I (Fig. 4). Consequently we focused on further characterizing ROS production by MitoPQ.

MitoPQ was several hundred-fold more potent than PQ at inducing hydrogen peroxide production from isolated mitochondria (Fig. 6B) and this hydrogen peroxide production was eliminated by preventing MitoPQ uptake with FCCP (Fig. 6C). To assess superoxide formation by MitoPQ more directly within mitochondria, we measured inactivation of the superoxide-sensitive matrix enzyme aconitase [30]. MitoPQ was several hundred-fold more potent at decreasing aconitase activity than PQ (Fig. 6D), and this inactivation was prevented by FCCP (Fig. 6E). We next monitored the relative amounts of monomeric and dimeric forms of peroxiredoxin 3 (Prdx3). This mitochondrial matrix antioxidant enzyme scavenges hydrogen peroxide to form a disulfide-bonded dimer, with the proportion in the monomeric form decreasing as mitochondrial hydrogen peroxide increases [39,40]. MitoPQ, but not PQ, caused the disappearance of monomeric Prdx3, consistent with increased matrix hydrogen peroxide, and this was prevented by FCCP (Fig. 6F). Together, these data support the accumulation of MitoPQ by energized mitochondria driving superoxide production within the matrix by redox cycling at complex I.

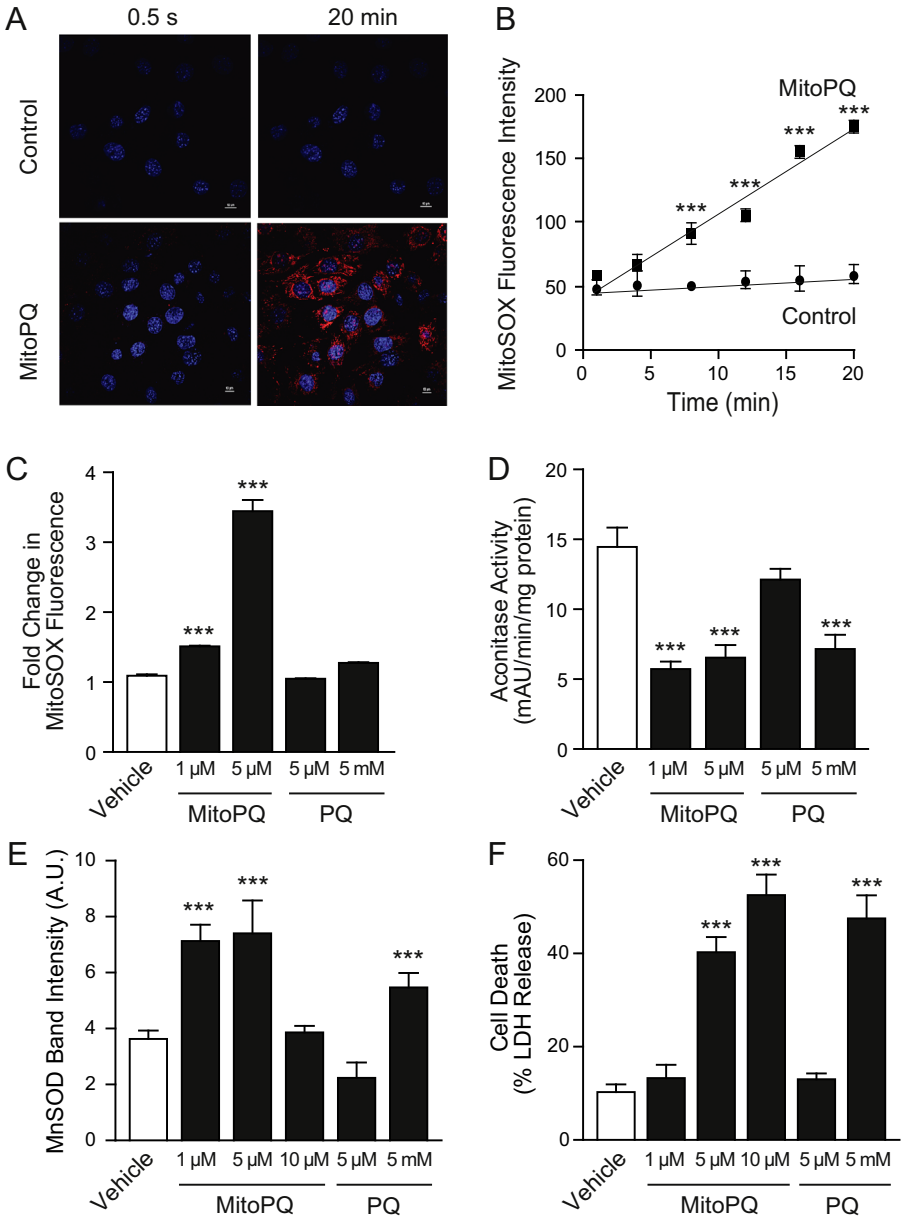


**Fig. 7.** MitoPQ increases reactive oxygen species production in mitochondria within cells. (A) Representative confocal image of superoxide production measured by MitoSOX fluorescence in C2C12 myoblasts 0.5 s or 20 min after addition of 10 μM MitoPQ or carrier. Red is oxidized MitoSOX and blue is DAPI nuclear staining. Scale bars = 10 μm. (B) Change in MitoSOX fluorescence over time in C2C12 cells treated with 5 μM MitoPQ. (C) Quantification of changes in MitoSOX fluorescence over 20 min in C2C12 cells treated with indicated concentrations of PQ or MitoPQ. (D) Aconitase activity in C2C12 myoblasts treated with PQ or MitoPQ for 6 h as indicated. (E) Increase in MnSOD protein levels in C2C12 myoblasts treated with indicated concentrations of MitoPQ or PQ for 12 h. Densitometry of MnSOD levels in western blots normalized to voltage dependent anion channel (VDAC) (Fig S2) was used to quantify MnSOD protein levels. (F) Cell death in HCT-116 cells measured as LDH release following incubation with PQ or MitoPQ for 24 h as indicated. Data in (B-F) are means ± S.D. of three or four independent experiments. $^{***}p < 0.001$ relative to control incubations (open bars) by Student's t test.

### *2.5. MitoPQ increases mitochondrial superoxide production within cells*

To see whether MitoPQ could stimulate superoxide production within mitochondria in cells, we used the increase of fluorescence of MitoSOX, which responds to elevated superoxide and hydrogen peroxide in the mitochondrial matrix [41]. MitoPQ increased MitoSOX fluorescence (Fig. 7A), and this oxidation increased over time (Fig. 7B). In contrast, PQ was unable to increase MitoSOX oxidation over this timescale, even at a thousand times greater concentration than used for MitoPQ (Fig. 7C). MitoPQ treatment for 6 h decreased aconitase activity, while the same concentration of PQ had no effect (Fig. 7D), also consistent with MitoPQ increasing superoxide production within mitochondria in cells.

To further assess MitoPQ superoxide production within mitochondria in cells, we measured MnSOD expression levels, which increases as an adaptation to elevated matrix superoxide [42,43]. MitoPQ increased MnSOD protein levels in a time- and dose-dependent manner, reaching a maximal induction of ~2-fold at 12 h (Fig. S2). Quantification by scanning densitometry showed that 1–5 μM MitoPQ increased MnSOD expression, while a thousand-fold higher PQ concentration was required to enhance expression to the same extent (Fig. 7E). Higher concentrations of MitoPQ decreased MnSOD protein levels, presumably due to mitochondrial

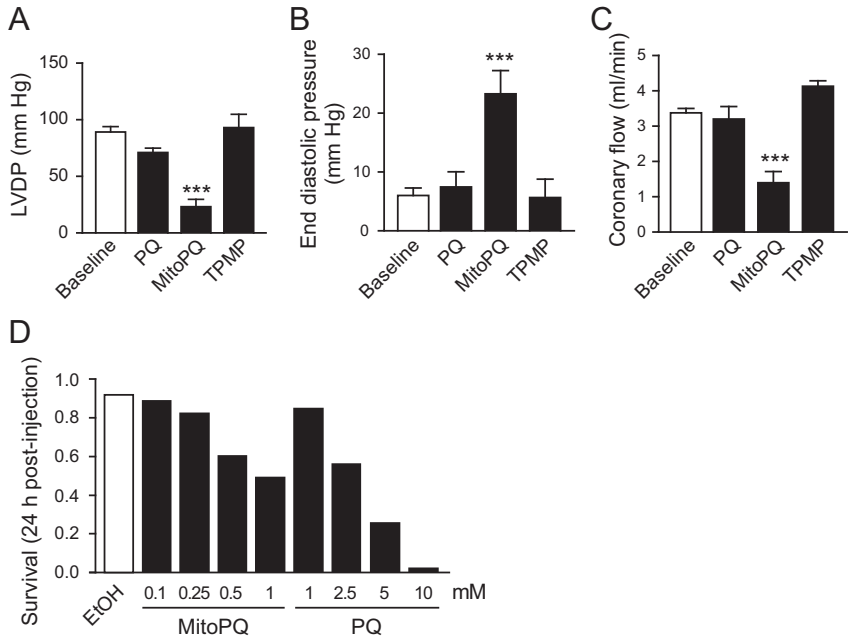


**Fig. 8.** Effects of MitoPQ in isolated hearts and *Drosophila in vivo*. (A-C) MitoPQ disrupts cardiac function in the isolated perfused heart. Mouse hearts were perfused in isovolumic Langendorff mode. After 20 min equilibration, hearts were randomized into three groups (each $n=6$), for 20 min treatment with 50 μM MitoPQ, PQ or TPMP and (A) left ventricular developed pressure (LVDP), (B) end diastolic pressure and (C) coronary flow were measured All data are means ± S.E.M. of $n=6$. *P* values were calculated using a two-tailed Student's t-test for pairwise comparisons. One-way analysis of variance (ANOVA) followed by Tukey's post-hoc test was used for multiple comparisons. (D). Wild-type 7 day old female flies were microinjected with MitoPQ or PQ (~75 nL over a range of concentrations). Survival at 24 h post-injection was assessed ($n=$ ~60–80 flies per condition).

damage by excessive superoxide production (Fig. 7E). This toxic effect of MitoPQ was confirmed by measuring cell viability, which showed that MitoPQ increased cell death, while several hundred-fold higher concentrations of PQ were required to generate comparable toxicity (Fig. 7F and Fig. S3). Together these data indicate that MitoPQ accumulates selectively within mitochondria in cells to generate superoxide that induces biological responses to elevated superoxide and, at higher concentrations, causes cell death.

### 2.6. MitoPQ disrupts mitochondrial function in the isolated perfused heart

We next assessed the effects of MitoPQ on the function of the isolated perfused heart. For this, we perfused beating mouse hearts in isovolumic Langendorff mode and functional parameters (systolic pressure, end diastolic pressure, coronary flow and perfusion pressure) were recorded throughout (Fig. 8A-C). Preliminary experiments showed that prolonged perfusion with 500 μM PQ was required to see toxic effects, while 5 μM MitoPQ was mildly damaging, therefore we assessed the effects of 50 μM MitoPQ in detail. After equilibration, hearts were randomized for perfusion with 50 μM MitoPQ, PQ, or TPMP (as a control for non-specific effects of lipophilic cations). MitoPQ decreased LVDP (Fig. 8A), increased end diastolic pressure (Fig. 8B) and decreased coronary flow (Fig. 8C), with no change in heart rate (data not shown). In contrast, the same concentrations of PQ or TPMP had no effect (Fig. 8A-C). These data are consistent with MitoPQ being far more damaging to heart function than PQ. This heart damage is due to its selective uptake by mitochondria within the heart and subsequent oxidative damage to the organelles leading to cell death and disruption to heart function.

### 2.7. MitoPQ is toxic to flies in vivo

To extend our study to whole organisms, we exposed wild-type *Drosophila melanogaster* to a single bolus of PQ or MitoPQ via microinjection, and monitored their survival (Fig. 9D). Over a range of concentrations, MitoPQ treatment was significantly more toxic to the flies than PQ (Fig. 8D). These data confirm that selective targeting of MitoPQ to mitochondria enhances toxicity relative to PQ *in vivo*.

### 2.8. Rationale for the poor uptake of PQ into mitochondria

Having shown that modification of PQ by conjugation to a hydrophobic TPP cation led to its accumulation by mitochondria, we next considered the reasons underlying the poor accumulation of PQ into mitochondria [19,20,29]. Lipophilic cations such as TPP are rapidly and extensively accumulated by energized mitochondria due to the membrane potential, but this does not occur for PQ, despite it being a cation [19,20,29]. Although the two charges on PQ are delocalized, the dication is very strongly solvated in water because the charged surface is solvent accessible (Fig. 9A). The related monocationic *N*-methylpyridinium (MBipy) also has a solvent accessible charge (Fig. 9A). On the other hand, steric congestion around the phosphorus atom of the TPP cation in triphenylmethylphosphonium (TPMP) shields the charge from the solvent, making the exposed surface much less polar than that of PQ (Fig. 9A). The increased solvation of PQ in water compared to TPP cation will make the energy for uptake across a membrane far greater for PQ and is the likely explanation for its poor uptake.

To obtain a more quantitative insight into the thermodynamics of the relative transport of PQ and TPMP from water into an apolar, lipophilic environment, we calculated the free energies for transfer from water to hexane for TPMP, MBipy and PQ and $Cl^-$. Hexane was chosen because it mimics the hydrophobic core of biological membranes, which is the most unfavourable environment through which cations must pass when crossing the membrane. One way of mitigating this energetic penalty is by cations forming ion pairs with $Cl^-$, the dominant anion present *in vivo* (Fig. 9B). The details of the calculations are given in the Supplementary Information and the results are summarized in Table 1. The relevant free

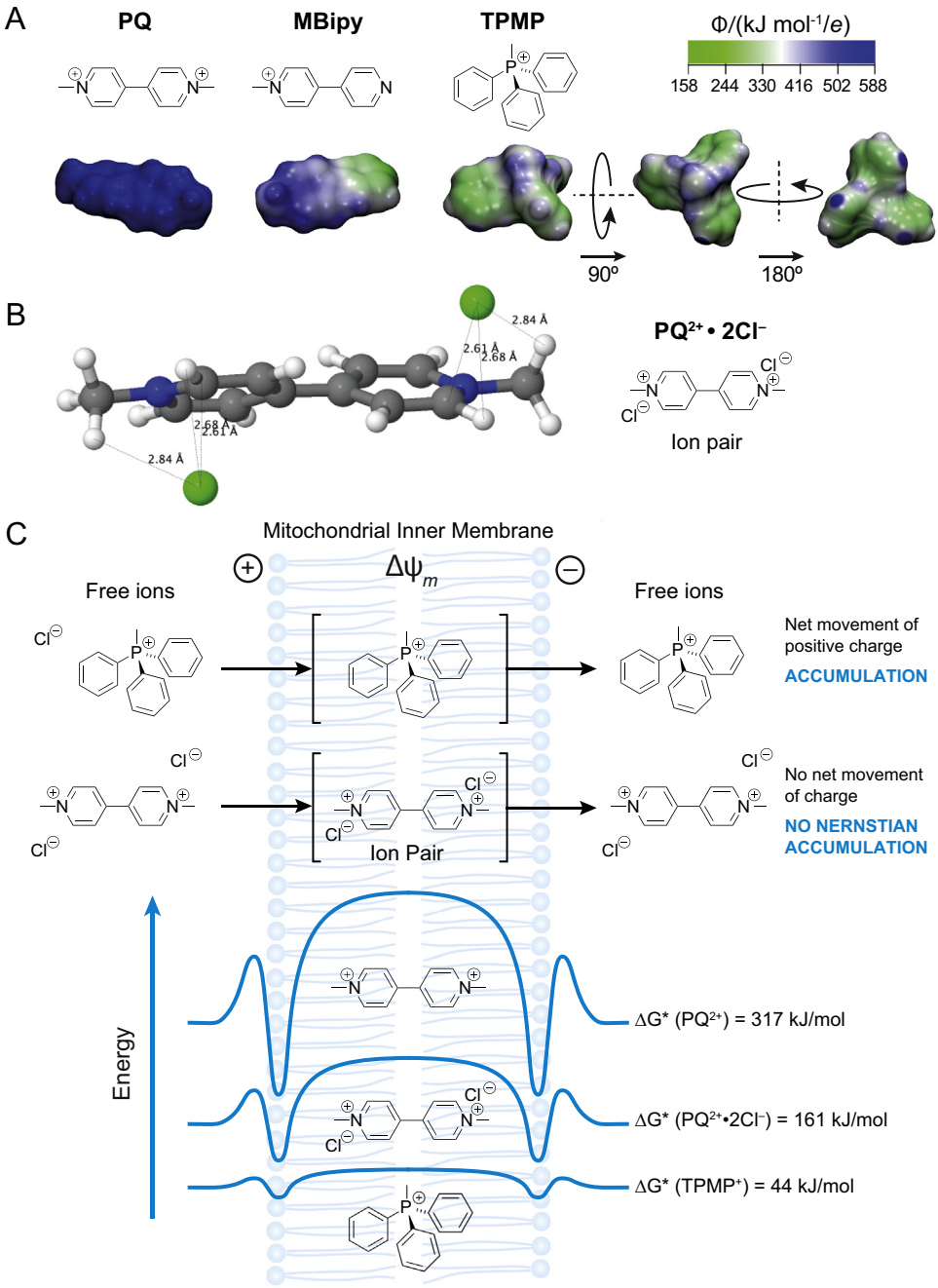


**Fig. 9.** Calculated molecular properties of ions and their consequences for mitochondrial uptake. (A) Solvent-accessible surfaces (SAS) of PQ, MBipy and TPMP (viewed from three different angles), colored by the molecular electrostatic potential, Φ. The scale is in kJ/mol per elementary charge *e*; that is, a positive unit charge that samples the SAS is (de)stabilized by the indicated amount. (B) DFT-optimized structure (in hexane) of the [$PQ^{2+}$ · 2 $Cl^-$] ion pair. (C) Schematic of the proposed ways in which TPMP and PQ cross the mitochondrial inner membrane. The upper section shows how TPMP and PQ cross the membrane while the lower section shows the relative energy profiles of PQ, the [$PQ^{2+}$ · 2 $Cl^-$] ion pair and TPMP calculated from Table 1.

energies for the comparison of free-ion *versus* ion-pair transfer of the cations from water to hexane, highlighted in bold in Table 1, are the free energy of transfer of the free ions and the sum of the free energies of transfer and ion-pairing. These calculations revealed two important effects: firstly, the energetic penalty for PQ to move into the non-aqueous hexane phase is more than seven times greater than that for TPMP; secondly, this penalty is significantly reduced when PQ transfers as a neutral ion pair with two chloride anions, while in contrast ion-pair formation increases the penalty for TPMP. The energy profile for transport of a lipophilic cation across a phospholipid bilayer has local minima close to the membrane surface and an energy maximum at the core of the membrane [23], and typical such profiles are shown in Fig. 9C. Thus, the relatively lipophilic TPMP ion (low overall charge, small surface charge, extended apolar surface area) can transfer as a free ion from water to hexane at moderate thermodynamic cost and does not benefit from ion pairing with $Cl^-$ (Fig. 9C). On the other hand, for the hydrophilic PQ ion (high overall charge, concentrated surface charge, little apolar surface area), it is thermodynamically prohibitive to transfer as a free ion. However, when paired with counter ions (even a small, hydrophilic one such as $Cl^-$), the cost is significantly reduced. Although hexane is more hydrophobic than

**Table 1**
Free energies[a] (in kJ mol$^{-1}$) for the transfer ($\Delta_t G^*$) of ions and ion pairs from water (aq) to hexane (Hex), and for ion-pair formation ($\Delta_{ip} G^*$) in either solvent.

| $S$ | $\Delta_t G^*(S, \text{aq}\rightarrow\text{Hex})$ | $\Delta_{ip} G^*(\text{aq})$ | $\Delta_{ip} G^*(\text{Hex})$ | $\Delta_{ip} G^*(\text{aq}) + \Delta_t G^*(S, \text{aq}\rightarrow\text{Hex})$ |
|---|---|---|---|---|
| $TPMP^+$ | **44** | | | |
| $MBipy^+$ | **100** | | | |
| $PQ^{2+}$ | **317** | | | |
| $Cl^-$ | 157 | | | |
| $[TPMP^+ \cdot Cl^-]$ | 39 | 19 | −143 | **58** |
| $[MBipy^+ \cdot Cl^-]$ | 71 | 16 | −170 | **88** |
| $[PQ^{2+} \cdot 2\ Cl^-]$ | 132 | 29 | −470 | **161** |

a. Calculated using density-functional theory with a continuum solvent model at the TPSS-D3/def2-TZVP+/SMD//TPSS-D3/def2-SVP+/COSMO level; see Supplementary Information for details.

the center of most membranes, exaggerating the effects described above, these calculations provide a plausible explanation for the poor accumulation of PQ into mitochondria [19,24]. Furthermore, these considerations suggest that PQ may cross the mitochondrial inner membrane as a neutral complex with two $Cl^-$ anions and so will not accumulate in response to the membrane potential, in contrast to TPMP. Additionally, even as an ion pair, the partitioning of PQ into the membrane is still thermodynamically very unfavorable (Fig. 9C).

This analysis may also shed light on some of the data shown in Fig. 5. There the mitochondrial uptake of MitoPQ, with a charge of +3, was not significantly different from that of the monocation TPMP. This was surprising, as the Nernst equation predicts far greater mitochondrial uptake for a trication over a monocation [24]. The explanation may be due to the ion pairing between the PQ moiety and two $Cl^-$ anions within the membrane (Fig. 9C), generating a neutral complex that is then transported into the mitochondria as a net monocation by the conjugated TPP. However, we note that DMV and DDV were also taken up by energized mitochondria, suggesting that the PQ moiety may also be able to cross the membrane as a singly charged complex with one $Cl^-$ anion, provided the overall molecule is sufficiently hydrophobic.

## 3. Conclusion

The ability to selectively increase mitochondrial superoxide production in the mitochondrial matrix in cells and *in vivo* would be very useful for investigating mitochondrial free radical production in health and disease. Existing methods to elevate mitochondrial superoxide use inhibitors of the electron transport chain, or redox cycling compounds such as PQ or menadione. However, the many side-effects of inhibiting mitochondrial respiration render results from these experiments almost impossible to interpret, while the uncertain intracellular location of redox cycling by PQ and menadione makes it hard to assign the effects to mitochondrial superoxide. Here we have developed a mitochondria-targeted viologen, MitoPQ that accumulates rapidly within mitochondria in cells and *in vivo* to increase matrix superoxide levels. While in this study the effects *in vivo* and in the perfused organ led to extensive damage, it will be possible to use lower, non-toxic levels of MitoPQ in the future to assess the effect of chronic elevation of superoxide. In addition, the increase in superoxide by MitoPQ, in the presence of nitric oxide, will also enable the effects of peroxynitrite *in vivo* to be assessed. The ability of MitoPQ to achieve rapid and specific increases in matrix superoxide will be useful in the further exploration in cells and *in vivo* of the nuanced roles of mitochondrial superoxide production in health and disease.

## Acknowledgements

This work was supported by the UK Medical Research Council (MC-A070-5PS30 and MC-A654-5QB90), the Biotechnology and Biological Sciences Research Council (BB/I012826/1), the University of Glasgow. We thank Sofia for timing her arrival after experiments were completed.

## Appendix A. Supplementary material

Supplementary data associated with this article can be found in the online version at http://dx.doi.org/10.1016/j.freeradbiomed.2015.08.021.

## References

[1] M.P. Murphy, How mitochondria produce reactive oxygen species, Biochem. J. 417 (2009) 1–13.
[2] B. Chance, H. Sies, A. Boveris, Hydroperoxide metabolism in mammalian organs, Physiol. Ress 59 (1979) 527–605.
[3] T. Finkel, Opinion: Radical medicine: treating ageing to cure disease, Nat Rev Mol. Cell Biol. 6 (2005) 971–976.
[4] E. Murphy, C. Steenbergen, Mechanisms underlying acute protection from cardiac ischemia-reperfusion injury, Physiol. Rev. 88 (2008) 581–609.
[5] D.C. Wallace, W. Fan, V. Procaccio, Mitochondrial energetics and therapeutics, Annu. Rev. Pathol 5 (2010) 297–348.
[6] T. Finkel, Signal transduction by reactive oxygen species, J. Cell Biol. 194 (2011) 7–15.
[7] Y. Collins, E.T. Chouchani, A.M. James, K.E. Menger, H.M. Cochemé, M. P. Murphy, Mitochondrial redox signalling at a glance, J. Cell Sci. 125 (2012) 801–806.
[8] Y.M. Janssen-Heininger, B.T. Mossman, N.H. Heintz, H.J. Forman, B. Kalyanaraman, T. Finkel, J.S. Stamler, S.G. Rhee, A. van der Vliet, Redox-based regulation of signal transduction: principles, pitfalls, and promises, Free Radic. Biol. Med. 45 (2008) 1–17.
[9] E.L. Robb, J.A. Stuart, Resveratrol interacts with estrogen receptor-beta to inhibit cell replicative growth and enhance stress resistance by upregulating mitochondrial superoxide dismutase, Free Radic. Biol. Med. 50 (2011) 821–831.
[10] Z. Chen, B. Siu, Y.S. Ho, R. Vincent, C.C. Chua, R.C. Hamdy, B.H. Chua, Overexpression of MnSOD protects against myocardial ischemia/reperfusion injury in transgenic mice, J. Mol. Cell. Card 30 (1998) 2281–2289.
[11] G.F. Kelso, A. Maroz, H.M. Cocheme, A. Logan, T.A. Prime, A.V. Peskin, C. C. Winterbourn, A.M. James, M.F. Ross, S. Brooker, C.M. Porteous, R. F. Anderson, M.P. Murphy, R.A.J. Smith, A mitochondria-targeted macrocyclic Mn(II) superoxide dismutase mimetic, Chemistry & Biology 19 (2012) 1237–1246.
[12] Y. Li, T.-T. Huang, E.J. Carlson, S. Melov, P.C. Ursell, J.L. Olson, L.J. Noble, M. P. Yoshimura, C. Berger, P.H. Chan, D.C. Wallace, C.J. Epstein, Dilated cardiomyopathy and neonatal lethality in mutant mice lacking mamganese superoxide dismutase, Nat. Genet. 11 (1995) 376–381.
[13] M.D. Williams, H. Van Remmen, C.G. Conrad, T.-T. Huang, C.J. Epstein, A. Richardson, Increased oxidative damage is correlated to altered mitochondrial function in heterozygous manganese superoxide dismutase knockout mice, J. Biol. Chem. 273 (1998) 28510–28515.
[14] H. Van Remmen, W. Qi, M. Sabia, G. Freeman, L. Estlack, H. Yang, Z. Mao Guo, T. T. Huang, R. Strong, S. Lee, C.J. Epstein, A. Richardson, Multiple deficiencies in antioxidant enzymes in mice result in a compound increase in sensitivity to oxidative stress, Free Radic. Biol. Med. 36 (2004) 1625–1634.
[15] S.G. Rhee, Cell signaling. $H_2O_2$, a necessary evil for cell signaling, Science 312 (2006) 1882–1883.
[16] A. Kim, W. Zhong, T.D. Oberley, Reversible modulation of cell cycle kinetics in NIH/3T3 mouse fibroblasts by inducible overexpression of mitochondrial manganese superoxide dismutase, Antiox. Redox Signal 6 (2004) 489–500.
[17] H.M. Hassan, Exacerbation of superoxide radical formation by paraquat, Meth. Enzymol 105 (1984) 523–532.
[18] H. Thor, M.T. Smith, P. Hartzell, G. Bellomo, S.A. Jewell, S. Orrenius, The metabolism of menadione (2-methyl-1,4-naphthoquinone) by isolated hepatocytes. A study of the implications of oxidative stress in intact cells, J. Biol. Chem. 257 (1982) 12419–12425.
[19] H.M. Cochemé, M.P. Murphy, Complex I is the major site of mitochondrial

superoxide production by paraquat, J. Biol. Chem. 283 (2008) 1786–1798.
[20] J.A. Birrell, M.S. King, J. Hirst, A ternary mechanism for NADH oxidation by positively charged electron acceptors, catalyzed at the flavin site in respiratory complex I, FEBS Letts 585 (2011) 2318–2322.
[21] S. Ramachandiran, J.M. Hansen, D.P. Jones, J.R. Richardson, G.W. Miller, Divergent mechanisms of paraquat, MPP+, and rotenone toxicity: oxidation of thioredoxin and caspase-3 activation, Toxicol. Sci. 95 (2007) 163–171.
[22] A.C. Cristovao, D.H. Choi, G. Baltazar, M.F. Beal, Y.S. Kim, The role of NADPH oxidase 1-derived reactive oxygen species in paraquat-mediated dopaminergic cell death, Antiox. Redox Signal 11 (2009) 2105–2118.
[23] M.F. Ross, G.F. Kelso, F.H. Blaikie, A.M. James, H.M. Cochemé, A. Filipovska, T. Da Ros, T.R. Hurd, R.A.J. Smith, M.P. Murphy, Lipophilic triphenylphosphonium cations as tools in mitochondrial bioenergetics and free radical biology, Biochemistry (Mosc) 70 (2005) 222–230.
[24] M.F. Ross, T. Da Ros, F.H. Blaikie, T.A. Prime, C.M. Porteous, I.I. Severina, V. P. Skulachev, H.G. Kjaergaard, R.A.J. Smith, M.P. Murphy, Accumulation of lipophilic dications by mitochondria and cells, Biochem. J. 400 (2006) 199–208.
[25] R.A.J. Smith, R.C. Hartley, H.M. Cochemé, M.P. Murphy, Mitochondrial pharmacology, Trends Pharmacol. Sci. 33 (2012) 341–352.
[26] R.A.J. Smith, R.C. Hartley, M.P. Murphy, Mitochondria-targeted small molecule therapeutics and probes, Antiox. Redox Signal 15 (2011) 3021–3038.
[27] C.C. Dahm, K. Moore, M.P. Murphy, Persistent S-nitrosation of complex I and other mitochondrial membrane proteins by S-nitrosothiols but not nitric oxide or peroxynitrite: Implications for the interaction of nitric oxide with mitochondria, J. Biol. Chem. 281 (2006) 10056–10065.
[28] M. Lucas, F. Solano, Coelenterazine is a superoxide anion-sensitive chemiluminescent probe: its usefulness in the assay of respiratory burst in neutrophils, Anal. Biochem. 206 (1992) 273–277.
[29] H.M. Cochemé, M.P. Murphy, The uptake and interactions of the redox cycler paraquat with mitochondria, Meth. Enzymol 456 (2009) 395–417.
[30] P.R. Gardner, Aconitase: sensitive target and measure of superoxide, Meth. Enzmol 349 (2002) 9–23.
[31] F.J. Sutherland, M.J. Shattock, K.E. Baker, D.J. Hearse, Mouse isolated perfused heart: characteristics and cautions, Clin. Exp. Pharm. Physiol 30 (2003) 867–878.
[32] T.M. Bass, R.C. Grandison, R. Wong, P. Martinez, L. Partridge, M.D. Piper, Optimization of dietary restriction protocols in *Drosophila. J. Gerontol. Series A, Biol*, Sci. Med. Sci. 62 (2007) 1071–1081.
[33] H.M. Cochemé, A. Logan, T.A. Prime, I. Abakumova, C. Quin, S.J. McQuaker, J. V. Patel, I.M. Fearnley, A.M. James, C.M. Porteous, R.A.J. Smith, R.C. Hartley, L. Partridge, M.P. Murphy, Using the mitochondria-targeted ratiometric mass spectrometry probe MitoB to measure $H_2O_2$ in living Drosophila. Nat, Protocols 7 (2012) 946–958.
[34] P.B. Pun, A. Logan, V. Darley-Usmar, B. Chacko, M.S. Johnson, G.W. Huang, S. Rogatti, T.A. Prime, C. Methner, T. Krieg, I.M. Fearnley, L. Larsen, D.S. Larsen, K.E. Menger, Y. Collins, A.M. James, G.D. Kumar, R.C. Hartley, R.A.J. Smith, M. P. Murphy, A mitochondria-targeted mass spectrometry probe to detect glyoxals: implications for diabetes, Free Rad. Biol. Med 67 (2014) 437–450.
[35] D.C. Hansen, J. Hadley, A. Read, E. Manwill, W. Pitt, D.R. Wheeler, A Comparison between dialkyl and monoalkyl viologens for use in direct-carbohydrate fuel cells, Electrochem. Soc. Trans. 41 (2011) 1737–1745.
[36] C.L. Bird, A.T. Kuhn, Electrochemistry of the viologens, Chem. Soc. Rev. 10 (1981) 49–82.
[37] N. Jordao, L. Cabrita, F. Pina, L.C. Branco, Novel bipyridinium ionic liquids as liquid electrochromic devices, Chemistry 20 (2014) 3982–3988.
[38] T. Akutagawa, T. Uchimaru, K.-I. Sakai, T. Hasegawa, T. Nakamura, Bidentated hydrogen bond from [O-H···N-N···H-O] to [O-…+H-N-N-H+…-O]structures in solids, J. Phys. Chem. B 107 (2003) 6248–6251.
[39] A.G. Cox, A.V. Peskin, L.N. Paton, C.C. Winterbourn, M.B. Hampton, Redox potential and peroxide reactivity of human peroxiredoxin 3, Biochemistry 48 (2009) 6495–6501.
[40] A.G. Cox, J.M. Pullar, G. Hughes, E.C. Ledgerwood, M.B. Hampton, Oxidation of mitochondrial peroxiredoxin 3 during the initiation of receptor-mediated apoptosis, Free Radic. Biol. Med. 44 (2008) 1001–1009.
[41] J. Zielonka, B. Kalyanaraman, Hydroethidine- and MitoSOX-derived red fluorescence is not a reliable indicator of intracellular superoxide formation: another inconvenient truth, Free Rad. Biol. Med 48 (2010) 983–1001.
[42] E. Larrea, O. Beloqui, M.A. Munoz-Navas, M.P. Civeira, J. Prieto, Superoxide dismutase in patients with chronic hepatitis C virus infection, Free Rad. Biol. Med 24 (1998) 1235–1241.
[43] Y. Hu, D.G. Rosen, Y. Zhou, L. Feng, G. Yang, J. Liu, P. Huang, Mitochondrial manganese-superoxide dismutase expression in ovarian cancer: role in cell proliferation and response to oxidative stress, J. Biol. Chem. 280 (2005) 39485–39492.